

GaAs photodetectors prepared by high-energy and high-dose nitrogen implantation

Martin Mikulics^{a)}

*Institute of Bio- and Nanosystems, Research Centre Jülich, D-52425 Jülich, Germany
and Institut für Hochfrequenztechnik, Technische Universität Braunschweig, Schleinitzstraße 22,
D-38106 Braunschweig, Germany*

Michel Marso,^{b)} Siegfried Mantl, and Hans Lüth

*Institute of Bio- and Nanosystems, Research Centre Jülich, D-52425 Jülich, Germany and Center of
Nanoelectronic Systems for Information Technology (CNI), Research Centre Jülich, D-52425 Jülich, Germany*

Peter Kordoš

*Institute of Electrical Engineering, Slovak Academy of Sciences, SK-84104 Bratislava
and Institute of Microelectronics, Slovak Technical University, SK-81219 Bratislava, Slovak Republic*

(Received 28 March 2006; accepted 19 July 2006; published online 28 August 2006)

The authors report on the fabrication and characterization of photodetectors based on nitrogen-ion-implanted GaAs and the annealing dynamics in these devices. An energy of 400 keV was used to implant N ions in a GaAs substrate at an ion concentration of $\sim 1 \times 10^{16} \text{ cm}^{-2}$. Dark current measurements as well as measurements under illumination show that the material properties rapidly change during the annealing process. Photodetectors based on nitrogen-implanted GaAs materials with annealing temperatures up to 400 °C exhibit a subpicosecond carrier lifetime up to 0.6 ps. These properties make nitrogen-ion-implanted GaAs an ideal material for ultrafast photodetectors, as alternative to low-temperature-grown GaAs. © 2006 American Institute of Physics. [DOI: 10.1063/1.2339907]

Implantation of various ions, such as As, Ga, Si, and O, into GaAs has been used to reduce trapping time and thus to achieve high-speed and broadband performance of various GaAs-based optoelectronic devices.^{1,2} Recently implantation of nitrogen into GaAs has been extensively studied with the main focus, so far, being on low-energy and high-dose implantation, besides investigations and applications of GaAs:N (Refs. 3–6) and preparation of $\text{GaN}_x\text{As}_{1-x}$ (Refs. 7 and 8) and GaN (Refs. 9 and 10) compounds. On the other hand, we recently reported on high-performance GaAs photomixers prepared on low-dose ($\sim 3 \times 10^{12} \text{ cm}^{-2}$) N⁺-implanted GaAs (Ref. 11) as an alternative to commonly used low-temperature GaAs. It is also known that the carrier trapping time in general decreases significantly with increased implantation dose. Subpicosecond values were reported for As⁺, Ga⁺, and Si⁺ implanted GaAs using 10^{16} – 10^{17} cm^{-2} doses.² However, properties of high-energy and high-dose N⁺-implanted GaAs have not been reported yet.

In this letter, the performance of metal-semiconductor-metal (MSM) photodetectors on N⁺-implanted GaAs using 400 keV and $1 \times 10^{16} \text{ cm}^{-2}$ implantation energy and dose, respectively, is described. Furthermore, the annealing dynamics of N⁺-implanted GaAs ($T_a = 200$ – 600 °C) is investigated.

The nitrogen implantation was performed into semi-insulating (100)-oriented GaAs wafers. The implantation energy and dose were 400 keV and $1 \times 10^{16} \text{ cm}^{-2}$, respectively. An annealing of N⁺-implanted GaAs samples at various temperatures from 200 to 600 °C for 10 min in nitrogen ambient

was performed in order to evaluate the annealing dynamics of nitrogen ions implanted into GaAs. Thereafter, the whole surface, except the designated area for the MSM structures, was coated with 400 nm SiO₂. On top of this insulator layer 10 mm long and 15 μm wide Ti/Au coplanar strip lines with thickness of 50/600 nm and 10 μm gap were fabricated using conventional photolithography and lift-off techniques. The MSM structures were formed as a part of the coplanar strip lines directly on the annealed N⁺-implanted GaAs material. For the sake of comparison, a MSM structure with the same geometry was fabricated also on nonannealed implanted material. Typical static current-voltage (*I*-*V*) characteristics of N⁺-implanted GaAs samples annealed at different temperatures and measured in the dark at 300 K are shown in Fig. 1. All samples exhibited Ohmic behavior and the dark current decreased rapidly with increased annealing temperature. The nonannealed and 200 °C annealed samples yielded high dark currents with resistivity of $\sim 1 \times 10^4 \Omega$. The break-

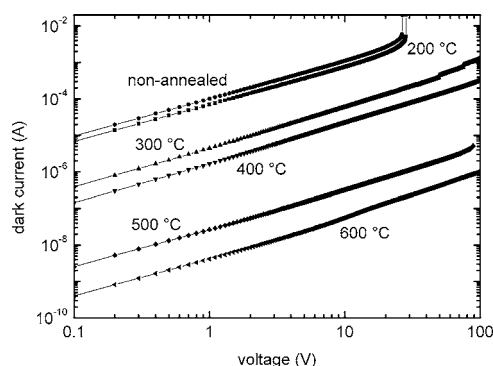


FIG. 1. Current-voltage characteristics in the dark for MSM photodetectors on nonannealed and annealed GaAs:N.

^{a)} Author to whom correspondence should be addressed; electronic mail: m.mikulics@fz-juelich.de

^{b)} Electronic mail: m.marso@fz-juelich.de

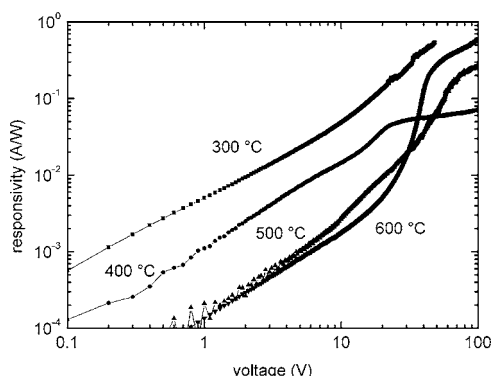


FIG. 2. Bias voltage dependence of responsivity for MSM photodetectors on annealed GaAs:N ($\lambda=850$ nm, $P_{\text{in}}=170$ μW).

down field was relatively low, $E_{\text{br}} \approx 30$ kV/cm. The resistivity of samples annealed at higher temperatures increased exponentially with annealing temperature, about one order of magnitude per 100 °C increase of the annealing temperature, without showing breakdown up to 100 V ($E_{\text{br}} > 100$ kV/cm). The samples annealed at 600 °C showed a resistivity of $2.5 \times 10^8 \Omega$, i.e., the dark current decreased more than four orders of magnitude compared to nonannealed material. An increase of the resistivity with annealing temperature was reported before on low-energy and low-dose implanted GaAs:N and was explained as being due to an increase of the density of N ions which act as electrically active traps.³

The photoelectric properties of GaAs:N MSM photodetectors were investigated at first by static I - V measurements under cw-laser illumination. The current responsivity $R = (I_{\text{total}} - I_{\text{dark}})/P_{\text{in}}$ as a function of the bias voltage, measured up to 100 V, is shown in Fig. 2. In the low-bias region (<20 V) the responsivity increased nearly linearly with bias and higher values were obtained on low-temperature-annealed material. This follows from a lower density of traps and thus higher gain of the photoconductor than in 500 and 600 °C annealed devices. At higher biases some deviation from linear R - V dependence was observed, more pronounced for high-temperature-annealed, i.e., higher resistive, samples. This might be due to space-charge effects at the contact-GaAs interface. Nevertheless, responsivity higher than 0.1 A/W can be achieved on 300 and 400 °C annealed materials at biases above 30 V. This is fully comparable or even higher than values previously reported on nitrogen⁴ or arsenic^{12,13} implanted GaAs-based photodetectors.

The lifetime of photogenerated carriers in GaAs:N was studied using femtosecond time-resolved reflectivity measurements by an all optical pump/probe system. A commercial Ti:sapphire laser with 100 fs wide pulses at 810 nm wavelength was used to investigate the carrier dynamics. Figure 3 shows the reflectivity change recorded on material annealed at 300, 400, and 600 °C. The GaAs:N materials exhibited very short carrier lifetime when annealed at lower temperatures. Values of 0.4 and 0.6 ps were extracted for 300 and 400 °C annealed samples, respectively. On the other hand, material annealed at 600 °C exhibited a slow decay in the reflectivity spectra and the approximated carrier lifetime is some hundreds of picoseconds. This indicates that two processes are involved in the annealing dynamics of high-energy (400 keV) and high-dose ($2 \times 10^{16} \text{ cm}^{-2}$) implanted GaAs:N. The first one is characterized by low influence on

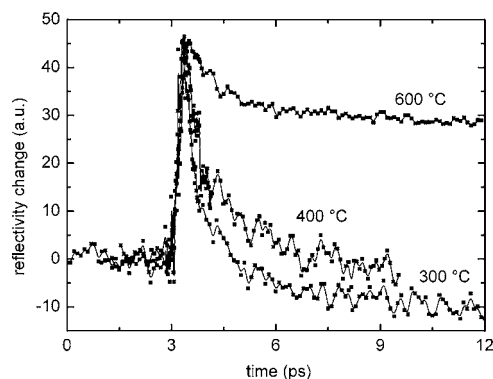


FIG. 3. Reflectivity measurement on annealed GaAs:N samples.

the carrier lifetime, i.e., the carrier lifetime increases slowly with the annealing temperature. In the second process the thermally activated traps have longer relaxation time but are created in sufficient density only at higher annealing temperatures. This seems to be similar to results reported on low-energy (160 keV) and high-dose ($2 \times 10^{15} \text{ cm}^{-2}$) implanted GaAs:N, in which two different trapping effects were observed in deep-level transient spectroscopy data on low- and high-temperature-annealed samples.³ The traps created at low annealing temperatures are responsible for the subpicosecond carrier lifetimes. On the other hand, the traps generated by the second process reduce the dark current and the responsivity in the high-temperature-annealed samples (Figs. 1 and 2), but their longer relaxation time is also responsible for the large increase of the carrier lifetime (Fig. 3). We verified this observation by photoresponse measurements on MSM photodetectors. Electrical transients were recorded by electro-optic sampling measurements, featuring ~ 100 fs resolution.¹⁴ The time-resolved photoresponse wave forms of our devices on 300, 400, and 600 °C annealed GaAs:N are shown in Fig. 4. The transients exhibit 0.7 and 1 ps full widths at half maximum with 0.5 and 0.8 ps rise times and $1/e$ decay times of 0.5 and 0.7 ps for 300 and 400 °C annealed samples, respectively. However, for 600 °C annealed sample, 1.3 ps rise time and a slow decay are observed, similar to the reflectivity measurement observation.

To conclude, we have fabricated ultrafast photodetectors based on nitrogen-implanted GaAs. Different annealing temperatures changed the dark current and photocurrent characteristics as well as carrier lifetime. The choice of the optimal annealing temperature allows achieving material suitable for the fabrication of ultrafast photodetectors. On the other hand,

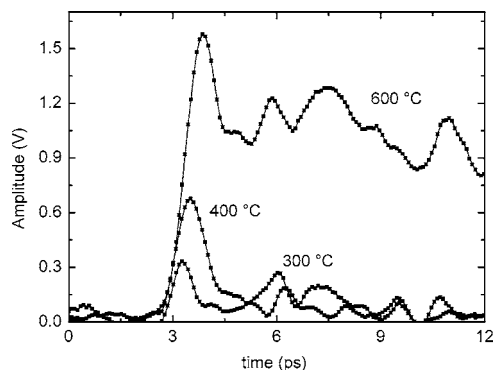


FIG. 4. Transient photoresponse of annealed GaAs:N implanted samples ($\lambda=810$ nm, $P_{\text{in}}=10$ mW, $V_B=50$ V).

it is possible to precisely engineer the material with exactly chosen carrier lifetime in a large range, from hundreds of femtoseconds up to nanoseconds. In this way it is possible to tune the properties of the prepared material for an optimum compromise between photodetector responsivity and speed.

The authors would like to acknowledge S. Wu, Xia Li, M. Khafizov, and R. Sobolewski from the Department of Electrical and Computer Engineering and the Laboratory for Laser Energetics, University of Rochester, Rochester, NY 14627-0231 for pump-probe measurements.

- ¹B. Salem, D. Morris, V. Aimez, J. Beerens, J. Beauvais, and D. Houde, *J. Phys.: Condens. Matter* **17**, 7327 (2005).
- ²A. Krotkus and J.-L. Coutaz, *Semicond. Sci. Technol.* **20**, S142 (2005).
- ³J. F. Chen, J. S. Wang, M. M. Huang, and N. C. Chen, *Appl. Phys. Lett.* **76**, 2283 (2000).
- ⁴M. Mikulics, M. Marso, P. Kordoš, S. Stanček, P. Kováč, X. Zheng, S. Wu, and R. Sobolewski, *Appl. Phys. Lett.* **83**, 1719 (2003).
- ⁵J. Wang, Z. Li, W. Xu, X. Guo, W. Cai, Q. Wang, X. Chen, and W. Lu,

- Appl. Phys. A: Mater. Sci. Process.* **79**, 1809 (2004).
- ⁶J. Wang, H. Mao, Z. Zhu, Q. Zhao, Z. Zhifeng, and W. Lu, *Appl. Surf. Sci.* **225**, 2186 (2005).
- ⁷K. M. Yu, W. Walukiewicz, J. W. Beeman, M. A. Scarpulla, O. D. Dubon, M. R. Pillai, and M. J. Aziz, *Appl. Phys. Lett.* **80**, 3958 (2002).
- ⁸S. Sinning, T. Dekorsy, and M. Helm, *IEEE Proc.: Optoelectron.* **151**, 361 (2004).
- ⁹K. C. Lo, H. P. Ho, K. Y. Fu, P. K. Chu, K. F. Li, and K. W. Cheah, *J. Appl. Phys.* **95**, 8178 (2004).
- ¹⁰S. Dhara, P. Magudapathy, R. Kesavamoorthy, S. Kalavathi, K. G. M. Nair, G. M. Hsu, L. C. Chen, K. H. Chen, K. Santhakumar, and T. Soga, *Appl. Phys. Lett.* **87**, 261915 (2005).
- ¹¹M. Mikulics, M. Marso, I. Cámara Mayorga, R. Güsten, S. Stanček, P. Kováč, S. Wu, X. Li, M. Khafizov, R. Sobolewski, E. A. Michael, R. Schieder, M. Wolter, D. Buca, A. Förster, P. Kordoš, and H. Lüth, *Appl. Phys. Lett.* **87**, 041106 (2005).
- ¹²Gong-Ru Lin and Ci-Ling Pan, *Appl. Phys. Lett.* **71**, 2901 (1997).
- ¹³T. A. Liu, G. R. Lin, Y. C. Lee, S. C. Wang, M. Tani, H. H. Wu, and C. L. Pan, *J. Appl. Phys.* **98**, 013711 (2005).
- ¹⁴M. Lindgren, M. Curie, C. Williams, T. Y. Hsiang, P. M. Fauchet, R. Sobolewski, S. H. Moffat, R. A. Hughes, J. S. Preston, and F. A. Hegman, *IEEE J. Sel. Top. Quantum Electron.* **2**, 668 (1996).